H.E.S.S. reveals a lack of TeV emission from the supernova remnant Puppis A
(Research Note)

H.E.S.S. Collaboration, A. Abramowski[1], F. Aharonian[2,3,4], F. Ait Benkhali[2], A.G. Akhperjanian[5,4], E.O. Angüner[6], M. Backes[7], S. Balenderan[8], A. Balzer[9], A. Barnacka[10,11], Y. Becherini[12], J. Becker Tjus[13], D. Berge[14], S. Bernhard[15], K. Bernlöhr[2,6], E. Birsin[6], J. Biteau[16,17], M. Böttcher[18], C. Boisson[19], J. Bolmont[20], P. Bordas[21], J. Bregeon[22], F. Brun[23], P. Brun[23], M. Bryan[9], T. Bulik[24], S. Carrigan[2], S. Casanova[25,2], P.M. Chadwick[8], N. Chakraborty[2], R. Chalme-Calvet[20], R.C.G. Chaves[22], M. Chrétien[20], S. Colafrancesco[26], G. Cologna[27], J. Conrad[28,29], C. Couturier[20], Y. Cui[21], I.D. Davids[18,7], B. Degrange[16], C. Deil[2], P. deWilt[30], A. Djannati-Ataï[31], W. Domainko[2], A. Donath[2], L.O'C. Drury[3], G. Dubus[32], K. Dutson[33], J. Dyks[34], M. Dyrda[25], T. Edwards[2], K. Egberts[35], P. Eger[2], P. Espigat[31], C. Farnier[28], S. Fegan[16], F. Feinstein[22], M.V. Fernandes[1], D. Fernandez[22], A. Fiasson[36], G. Fontaine[16], A. Förster[2], M. Füßling[35], S. Gabici[31], M. Gajdus[6], Y.A. Gallant[22], T. Garrigoux[20], G. Giavitto[37], B. Giebels[16], J.F. Glicenstein[23], D. Gottschall[21], M.-H. Grondin[38], M. Grudzińska[24], D. Hadasch[15], S. Häffner[39], J. Hahn[2], J. Harris[8], G. Heinzelmann[1], G. Henri[32], G. Hermann[2], O. Hervet[19], A. Hillert[2], J.A. Hinton[33], W. Hofmann[2], P. Hofverberg[2], M. Holler[35], D. Horns[1], A. Ivascenko[18], A. Jacholkowska[20], C. Jahn[39], M. Jamrozy[10], M. Janiak[34], F. Jankowsky[27], I. Jung-Richardt[39], M.A. Kastendieck[1], K. Katarzyński[40], U. Katz[39], S. Kaufmann[27], B. Khélifi[31], M. Kieffer[20], S. Klepser[37], D. Klochkov[21], W. Kluźniak[34], D. Kolitzus[15], Nu. Komin[26], K. Kosack[23], S. Krakau[13], F. Krayzel[36], P.P. Krüger[18], H. Laffon[38], G. Lamanna[36], J. Lefaucheur[31], V. Lefranc[23], A. Lemière[31], M. Lemoine-Goumard[38], J.-P. Lenain[20], T. Lohse[6], A. Lopatin[39], C.-C. Lu[2], V. Marandon[2], A. Marcowith[22], R. Marx[2], G. Maurin[36], N. Maxted[22], M. Mayer[35], T.J.L. McComb[8], J. Méhault[38,41], P.J. Meintjes[42], U. Menzler[13], M. Meyer[28], A.M.W. Mitchell[2], R. Moderski[34], M. Mohamed[27], K. Morå[28], E. Moulin[23], T. Murach[6], M. de Naurois[16], J. Niemiec[25], S.J. Nolan[8], L. Oakes[6], H. Odaka[2], S. Ohm[37], B. Opitz[1], M. Ostrowski[10], I. Oya[37], M. Panter[2], R.D. Parsons[2], M. Paz Arribas[6], N.W. Pekeur[18], G. Pelletier[32], P.-O. Petrucci[32], B. Peyaud[23], S. Pita[31], H. Poon[2], G. Pühlhofer[21], M. Punch[31], A. Quirrenbach[27], S. Raab[39], I. Reichardt[31], A. Reimer[15], O. Reimer[15], M. Renaud[22], R. de los Reyes[2], F. Rieger[2], C. Romoli[3], S. Rosier-Lees[36], G. Rowell[30], B. Rudak[34], C.B. Rulten[19], V. Sahakian[5,4], D. Salek[43], D.A. Sanchez[36], A. Santangelo[21], R. Schlickeiser[13], F. Schüssler[23], A. Schulz[37], U. Schwanke[6], S. Schwarzburg[21], S. Schwemmer[27], H. Sol[19], F. Spanier[18], G. Spengler[28], F. Spies[1], Ł. Stawarz[10], R. Steenkamp[7], C. Stegmann[35,37], F. Stinzing[39], K. Stycz[37], I. Sushch[6,18], J.-P. Tavernet[20], T. Tavernier[31], A.M. Taylor[3], R. Terrier[31], M. Tluczykont[1], C. Trichard[36], K. Valerius[39], C. van Eldik[39], B. van Soelen[42], G. Vasileiadis[22], J. Veh[39], C. Venter[18], A. Viana[2], P. Vincent[20], J. Vink[9], H.J. Völk[2], F. Volpe[2], M. Vorster[18], T. Vuillaume[32], S.J. Wagner[27], P. Wagner[6], R.M. Wagner[28], M. Ward[8], M. Weidinger[13], Q. Weitzel[2], R. White[33], A. Wierzcholska[25], P. Willmann[39], A. Wörnlein[39], D. Wouters[23], R. Yang[2], V. Zabalza[2,33], D. Zaborov[16], M. Zacharias[27], A.A. Zdziarski[34], A. Zech[19], and H.-S. Zechlin[1]

(Affiliations can be found after the references)

ABSTRACT

Context: Puppis A is an interesting ~4 kyr-old supernova remnant (SNR) that shows strong evidence of interaction between the forward shock and a molecular cloud. It has been studied in detail from radio frequencies to high-energy (HE, 0.1-100 GeV) γ-rays. An analysis of the *Fermi*-LAT data has shown an extended HE γ-ray emission with a 0.2-100 GeV spectrum exhibiting no significant deviation from a power law, unlike most of the GeV-emitting SNRs known to be interacting with molecular clouds. This makes it a promising target for imaging atmospheric Cherenkov telescopes (IACTs) to probe the γ-ray emission above 100 GeV.

Aims: Very-high-energy (VHE, $E \geq 0.1$ TeV) γ-ray emission from Puppis A is for the first time searched for with the High Energy Stereoscopic System (H.E.S.S.).

Methods: Stereoscopic imaging of Cherenkov radiation from extensive air showers is used to reconstruct the direction and energy of the incident γ-rays in order to produce sky images and source spectra. The profile likelihood method is applied to constrain the existence of a potential break or cutoff in the photon spectrum.

Results: The analysis of the H.E.S.S. data does not reveal any significant emission towards Puppis A. The derived upper limits on the differential photon flux imply that its broadband γ-ray spectrum must exhibit a spectral break or cutoff. By combining *Fermi*-LAT and H.E.S.S. measurements, the 99% confidence level upper limits on such a cutoff are found to be 450 and 280 GeV, assuming a power law with a simple exponential and a sub-exponential cutoff, respectively. It is concluded that none of the standard limitations (age, size, radiative losses) on the particle acceleration mechanism, assumed to be still on-going at present, can explain the lack of VHE signal. The scenario in which particle acceleration has ceased some time ago is considered as an alternative explanation. The HE/VHE spectrum of Puppis A could then exhibit a break of non-radiative origin, (as observed in several other interacting SNRs, albeit at somewhat higher energies) owing to the interaction with dense and neutral material in particular towards the northeastern region.

Key words. Gamma rays: ISM - ISM: individual (Puppis A) - radiation mechanisms: nonthermal - ISM: cosmic rays - acceleration of particles

1. Introduction

Supernova remnants (SNRs) have long been considered as the main sources of Galactic cosmic rays (CRs, Ginzburg & Syrovatskii 1964). Direct measurements of CRs from SNRs are impossible due to Galactic magnetic fields, but γ-rays can provide an indirect signature of their presence (see e.g. Reynolds 2008, for a review). On one hand, several middle-aged SNRs interacting with molecular clouds (MCs) have been observed with the *Fermi* Large Area Telescope (*Fermi*-LAT) and Astro-Rivelatore Gamma a Immagini Leggero (*AGILE*) telescope as luminous high-energy (HE, $0.1-100$ GeV) γ-ray sources. The strong HE γ-ray emission from these sources is thought to arise from neutral pion decay subsequent to the interactions between accelerated CR particles and the dense gas, and whose unique spectral feature, referred to as the pion bump at ~ 200 MeV, was recently revealed in two such SNRs with *Fermi*-LAT (Ackermann et al. 2013). Some examples are W28 (Abdo et al. 2010a), W51C (Abdo et al. 2009), W44 (Abdo et al. 2010b), and IC 443 (Abdo et al. 2010c), which furthermore all exhibit power-law spectral breaks in the $1-20$ GeV range. As a consequence of these breaks, the associated very-high-energy (VHE, $E \geq 0.1$ TeV) emission is usually soft and faint (e.g. Albert et al. 2007; Aharonian et al. 2008). On the other hand, young, shell-type SNRs, with bright and hard spectra in the VHE domain (such as RX J1713.7−3946, Aharonian et al. 2007) and without clear evidence for cloud interaction, exhibit hard and relatively faint spectra in the HE domain (Abdo et al. 2011). In these cases, inverse Compton (IC) emission from accelerated electrons naturally explains the observed γ-ray emission (e.g. Lee et al. 2012).

Puppis A (G260.4−3.4) represents an interesting case in between the two above-mentioned SNR categories. At a distance of 2.2 ± 0.3 kpc[1] (Reynoso et al. 2003), it is a well-studied Galactic SNR in most energy bands, from radio to HE γ-rays. It is one of the three oxygen-rich SNRs (Winkler & Kirshner 1985) known today in the Galaxy. This, together with the presence of a central compact object (CCO; Becker et al. 2012, and references therein), strongly supports the idea that Puppis A originates from a core-collapse SN explosion. Based on the motions of both optical filaments and CCO, its age is estimated to be (4450 ± 750) yr (Becker et al. 2012), implying that the SNR is currently in the Sedov-Taylor evolutionary phase (see e.g. Chevalier 1977). The strong X-ray emission from Puppis A is mostly dominated by the shock-heated interstellar medium (ISM, e.g. Hwang et al. 2005), except for some isolated O-Ne-Mg-rich features associated with the SN ejecta (Hwang et al. 2008; Katsuda et al. 2008, 2010) the kinematics of which have been well measured (Katsuda et al. 2013, and references therein). The SNR also has another interesting characteristic: together with W49B (Abdo et al. 2010d) and G349.7+0.2 (Lazendic et al. 2010), it is amongst the youngest Galactic SNRs known to be interacting, at several locations throughout the shell, with dense gas seen as a complex of H I and CO clouds surrounding most of the SNR (Dubner & Arnal 1988; Reynoso et al. 1995; Dubner et al. 2013). In particular, spectro-imaging X-ray studies towards the so-called bright eastern knot (BEK) have presented evidence for a shock-cloud inter-

action (Hwang et al. 2005). Recent high-resolution X-ray observations of the whole SNR (Dubner et al. 2013) have confirmed the presence of a decreasing gradient in the emission from northeast to southwest and also revealed a highly structured and filamentary morphology with unprecedented detail, indicating that Puppis A is evolving in an inhomogeneous, knotty ISM. Observations with *Spitzer* have shown a clear correlation between infrared (IR) and X-rays at all spatial scales, demonstrating that the thermal IR emission arises from dust collisionally heated by the hot, shocked plasma (Arendt et al. 2010).

Hewitt et al. (2012) have reported the detection of Puppis A in the HE γ-ray domain with the *Fermi*-LAT. Its luminosity of $2.7 \times 10^{34}(d/2.2 \text{ kpc})^2$ erg s^{-1} in the $1-100$ GeV band is slightly higher than those of the low-luminosity, HE-emitting SNRs such as Cygnus Loop, S147 and HB21 (Reichardt et al. 2012 and references therein), and about a factor ten lower than those measured from the archetypal SNRs known to be interacting with MCs (Abdo et al. 2009, 2010c,d). The morphology of the HE γ-ray emission is well described by a uniform disc of radius $0.38° \pm 0.04°$ and compatible with the radio and X-ray morphologies. The HE γ-ray spectrum is well described by a power law (PL) with no indication of a break or cutoff, and a spectral variation at the $\sim 2\sigma$ level between the eastern and the western hemispheres was found Such a PL HE spectrum, together with a hint of a radio break at ~ 40 GHz in the WMAP data (Hewitt et al. 2012), makes Puppis A quite peculiar with respect to most of the HE-emitting SNRs. Puppis A can be considered as an intermediate case between the young, isolated and bright VHE γ-ray emitting SNRs and the middle-aged, bright HE γ-ray emitting ones interacting with MCs. In order to probe its emission in the VHE domain, observations towards Puppis A obtained with the High Energy Stereoscopic System (H.E.S.S.) are reported in this article.

2. Observations and analysis

2.1. H.E.S.S. observations and analysis results

H.E.S.S. is an array of five imaging atmospheric Cherenkov telescopes (IACTs) located in Namibia and designed to detect VHE γ-rays (Bernlöhr et al. 2003). The fifth telescope (28-m diameter) has been operating since September 2012, but the data exploited here have been taken from 2005 to 2013 with the four-telescope array only. In this configuration, the instrument covers a field-of-view of $5°$. The primary particle direction and energy are reconstructed above a threshold of ~ 100 GeV with an angular resolution of $\sim 0.1°$ and energy resolution of $\sim 15\%$, (e.g. Aharonian et al. 2006a). The whole dataset on Puppis A amounts to 24 h including 17 h of dedicated observations taken using the *wobble* mode and 7 h of runs towards nearby sources in the Vela region (in particular, Vela X, Aharonian et al. 2006b; Abramowski et al. 2012). These observations were performed at zenith angles between $18°$ and $45°$ with a median value of $22°$, and a median offset from the source of $1.0°$.

Data were analysed with the Model Analysis as described in de Naurois & Rolland (2009) and using *Standard cuts*[2]. The main analysis results were confirmed with an independent data calibration chain and a multivariate analysis method (Ohm et al. 2009). The resulting energy threshold of the main analysis, conservatively defined as the energy above which the acceptance is larger than 15% of its maximum value, is $E_{\text{th}} = 0.26$ TeV.

Send offprint requests to: Diane Fernandez
e-mail: `diane.fernandez@lupm.univ-montp2.fr`
Igor Oya
e-mail: `igor.oya.vallejo@desys.de`

[1] Although a smaller distance of 1.3 kpc, with large uncertainties of +0.6/-0.8 kpc, has been previously determined by Woermann et al. (2000) based on OH line observations, a distance of 2.2 kpc is assumed throughout this paper.

[2] The H.E.S.S. *ParisAnalysis version 0-8-24* software with *Prod26 DSTs* was used.

The analysis ON-region (i.e. signal integration region) was defined as a circular region of radius 0.38°, centred on $\alpha_{J2000} = 08^h22^m40^s.8$, $\delta_{J2000} = -42°55'48''.0$, to match the best-fit values of the HE γ-ray emission extent and position measured with the *Fermi*-LAT[3]. The statistical significance of a potential VHE γ-ray emission from Puppis A is determined by using equation (17) in Li & Ma (1983) after background subtraction with the reflected background method (Berge et al. 2007). No significant signal was found within the ON-region. In total, 8 excess counts were measured, corresponding to a significance of 0.1σ. Similar analyses have been performed for two half-disc regions corresponding to the eastern and western hemispheres as defined in Hewitt et al. (2012). Figure 1 shows an image of the γ-ray excess counts, where the background level is estimated following the template background method and cross-checked with the ring background method (Berge et al. 2007), together with the ON-region and contours of the radio continuum emission at 1.4 GHz (Castelletti et al. 2006).
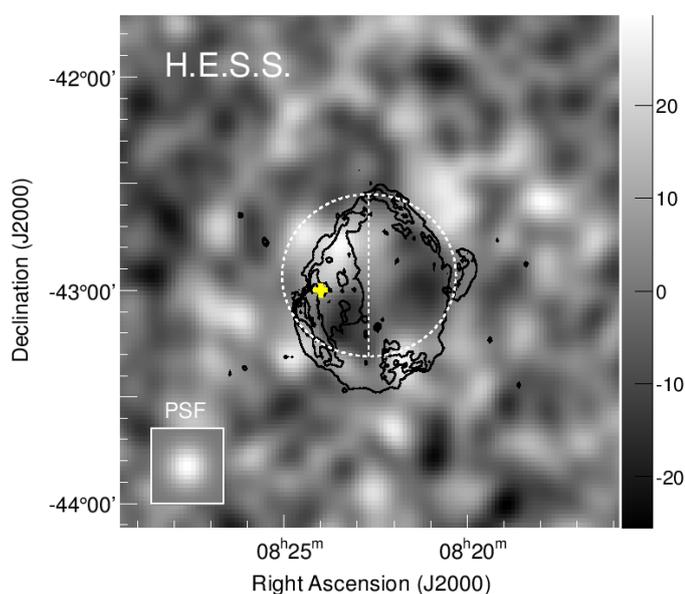
Fig. 1. Image of the H.E.S.S. γ-ray excess centred on the Puppis A SNR. The excess was smoothed with a Gaussian kernel of width 0.06° corresponding to the H.E.S.S. angular resolution (68% containment radius) for this analysis (shown in the bottom left inset). The colour scale represents the excess counts per surface area of $\pi(0.06°)^2$. The circular analysis region of radius 0.38°, matching the *Fermi*-LAT best-fit morphological model, is shown as a dashed circle. The two hemispheres are separated by a dashed line along the north/south axis in celestial coordinates. The black contours represent the 1.4 GHz continuum emission (Castelletti et al. 2006) at the 5, 10, 20 and 50 mJy/beam levels. The yellow cross indicates the position of the BEK (Hwang et al. 2005).

Following the method of Feldman & Cousins (1998), differential flux upper limits (ULs) at the 99% confidence level (CL) and for a spectral index $\Gamma = 2.1$ (as measured with *Fermi*-LAT, Hewitt et al. 2012) were extracted in the 0.26–10 TeV energy range within the circular and the two half-disc ON-regions. Note that these ULs are not very sensitive to the choice of the photon index; assuming $\Gamma = 3$ instead changes the values by less than 5%. To ensure that these ULs account for the full source emission, they have been corrected for the underestimation caused

by events reconstructed outside the analysis regions due to the H.E.S.S. point spread function (PSF). By convolving a disc of 0.38° radius with the H.E.S.S. PSF, the flux outside of the ON-region was estimated to be 10% of the total flux. The H.E.S.S. ULs do not vary by more than 10% by changing the integration radius between 0.35° and 0.48°. The resulting H.E.S.S. ULs are shown in Fig. 2 together with the *Fermi*-LAT spectra.
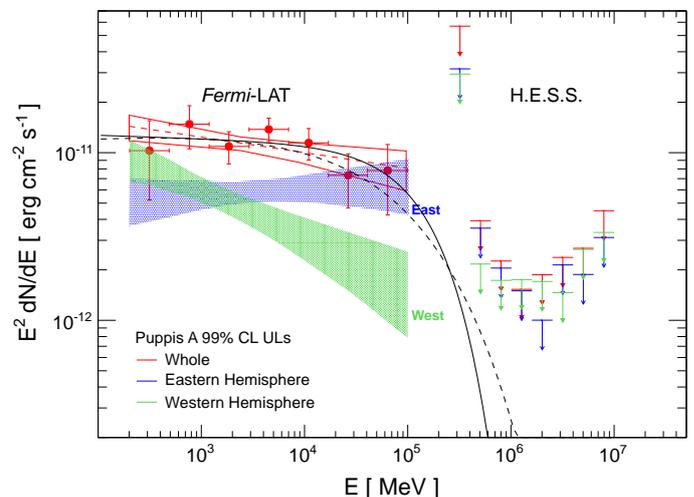

Fig. 2. H.E.S.S. 99% CL upper limits on the differential flux (arrows) together with the *Fermi*-LAT spectra from Puppis A, as reported in Hewitt et al. (2012). Red, blue and green symbols correspond to *Fermi*-LAT and H.E.S.S. measurements for the whole SNR, the eastern and western hemisphere, respectively. The data points show the LAT fluxes and 1 σ statistical and systematic errors, whilst the bow-tie areas define the 68% CL bands. The solid and dashed lines indicate the preferred γ-ray spectra for the exponential and sub-exponential cutoff models, respectively.

While the H.E.S.S. ULs derived from the western hemisphere are not constraining, owing to a steeper HE spectrum, those from the eastern hemisphere and from the whole SNR exclude the possibility that their respective PL spectra extend up to the VHE domain at more than the 99% CL. This indicates the existence of a spectral feature (break or cutoff) at intermediate energies, i.e. between the HE and VHE domains.

2.2. Constraints on the CR particle spectrum

Presuming that the accelerated particle spectra are PLs with exponential cutoffs as predicted by the diffusive shock acceleration (DSA) mechanism (e.g. Krymskii 1977; Blandford & Ostriker 1978; Bell 1978a,b), the γ-ray spectrum resulting from the different emission processes should also follow a PL with exponential cutoff: $dN/dE = N_0 E^{-\Gamma} e^{-(E/E_{cut})^\beta}$, where E_{cut} is the cutoff energy and β defines the spectral shape in the cutoff region. To evaluate the existence of such a cutoff energy in the spectrum of the whole SNR[4], a likelihood estimator $\mathcal{L}$ was defined as the combination of the likelihoods from the *Fermi*-LAT data points and H.E.S.S. measurements. The *Fermi*-LAT likelihood value was estimated by computing χ^2 from the available data points and 1σ errors. The H.E.S.S. likelihood is calculated by comparing the number of detected excess events (following Poisson statistics) with the expected number in each reconstructed energy bin. To cover a wide range of physically possible scenarios,

---

[3] The HE spectral parameters have been obtained with the ROSAT X-ray template. However, as shown in Table 3 of Hewitt et al. (2012), those derived under the assumption of a uniform disc are fully compatible.

[4] Since no *Fermi*-LAT spectral points are available for the hemispheres, no ULs on a cutoff or break have been derived.

two values for the β parameter were chosen: $\beta = 1$ (defining the *exponential cutoff model* hereafter) corresponds to the most commonly used case and $\beta = 0.5$ (defining the *sub-exponential cutoff* model hereafter) is more physically motivated in both leptonic (under the assumption that electrons suffer from SC losses and that diffusion proceeds in Bohm regime, Zirakashvili & Aharonian 2007) and hadronic (for a proton spectrum exhibiting a simple exponential cutoff, Kelner et al. 2006) scenarios. The method used to derive the exclusion domain of E_{cut} is based on a likelihood ratio test statistic (Rolke et al. 2005):

$$\Lambda(E_{cut_0}) = \frac{\sup\limits_{\theta} \mathcal{L}(E_{cut_0}, \theta)}{\sup\limits_{E_{cut}, \theta} \mathcal{L}(E_{cut}, \theta)}, \quad (1)$$

where E_{cut_0} is the tested hypothesis and E_{cut} all the allowed values. The unknown spectral index Γ and normalisation N_0 are considered as nuisance parameters under the θ variable. The profile of the log-likelihood ratio test statistic $-2\ln\Lambda$ has an approximate χ^2 distribution with 1 degree of freedom (Rolke et al. 2005). The minimum is reached at around ~ 55 GeV and 150 GeV for $\beta = 0.5$ and 1, respectively. Below these energies, $-2\ln\Lambda$ increases rapidly because of the constraints imposed by the *Fermi*-LAT detection. Above that, the H.E.S.S. data become more constraining and lead to an increase of the $-2\ln\Lambda$ value. The 99% CL ULs on the cutoff energy correspond to 280 and 450 GeV for $\beta = 0.5$ and 1, respectively[5].

Broken PL spectra have been observed in several SNRs interacting with MCs (e.g. Abdo et al. 2010a,b), and this could also be the case for Puppis A. A spectral index variation $\Delta\Gamma \sim 1$ can be explained by radiative cooling of electrons or escape of protons in the case of a SNR encountering a dense and neutral medium (Malkov et al. 2012). The derived UL on the sub-exponential cutoff energy (280 GeV) can be used as a conservative UL on the energy of any spectral break as long as $\Delta\Gamma \lesssim 1$.

3. Discussion

Throughout the SNR evolution, particles are accelerated at the forward shock up to a maximal energy E_{max}, typically determined by the SNR's finite age, finite size, or radiative losses. These effects become relevant when the characteristic timescales are of the order of the acceleration timescale and lead to cutoffs in the spectra of accelerated particles residing in the SNR. Additionally, a radiative spectral break can also be present at the particle energy E_{break} for which the radiative loss timescales equal the SNR age. The conservative ULs on the cutoff energy in the γ-ray spectrum derived from the *Fermi*-LAT and H.E.S.S. measurements translate into ULs on E_{max} of ~ 2 TeV, ~ 3 TeV or ~ 5 TeV depending on whether the γ-ray emission results from Bremsstrahlung (Br), IC or proton-nucleus interactions (e.g. p-p) radiation mechanisms. These limits can in turn be compared with the expectations from DSA theory taken in its simplest form and applied to the case of Puppis A whose main parameters are an age of ~ 4500 yr (Becker et al. 2012), a shock radius $R_{sh} = 15$ pc (for $R_{sh} = 24'$ at 2.2 kpc), and a shock velocity v_{sh} ranging from 700 to 2500 km s^{-1}. The latter velocity value was estimated by Katsuda et al. (2013) based on the electron temperatures and ionization timescales in the ejecta knots, whilst the former was derived from the shock temperature of

~ 0.7 keV (Hwang et al. 2008) by assuming full equipartition of the shock energy between ions and electrons. These shock velocity estimates concern the northeastern (NE) region of the SNR, which is also the region coincident with the bulk of GeV emission. Based on these SNR parameters, constraints on the magnetic field and ISM density can be derived and compared to independent estimates (Hewitt et al. 2012; Dubner et al. 2013). In these calculations, the acceleration is assumed to proceed in a steady-state manner from the SN until now, and the derived constraints are implicitly considered as having been constant. Assuming Bohm diffusion, the acceleration timescale[6] and the diffusion coefficient are $\tau_{acc} = (3 \times 10^3 \text{ yr}) E_{TeV} B_{\mu G}^{-1} v_{sh,3}^{-2}$ and $D(E_{TeV}) = (3.3 \times 10^{25} \text{ cm}^2 \text{ s}^{-1}) E_{TeV} B_{\mu G}^{-1}$ (Parizot et al. 2006), where $B_{\mu G}$ is the downstream magnetic field in units of μG, E_{TeV} the particle energy in units of TeV and $v_{sh,3}$ the shock velocity in units of 10^3 km s^{-1}. Synchrotron (syn), p-p and Br radiative loss timescales are $\tau_{syn} \simeq (2.1 \times 10^7 \text{ yr}) B_{\mu G}^{-2} E_{TeV}^{-1}$ (Parizot et al. 2006), $\tau_{p-p} \simeq (5.3 \times 10^7 \text{ yr}) n_0^{-1}$ and $\tau_{br} \simeq (3.3 \times 10^7 \text{ yr}) n_0^{-1}$ (Gabici et al. 2009), with n_0 the ISM density in units of cm^{-3}, and $B_{\mu G}$ is the downstream magnetic field in units of μG. The derived constraints are shown in Table 1.

Table 1. Constraints on $B_{\mu G}$ and n_0 based on standard DSA predictions (assuming Bohm diffusion) and the ULs on the maximum particle energy derived from the *Fermi*-LAT and H.E.S.S. measurements.

Scenario	Constraints		
Radiative losses τ_{rad}:	($\tau_{acc} > \tau_{rad}$)		
τ_{p-p}	$B_{\mu G}$	$<$	$1.1 \times 10^{-4} n_0 E_{max}$
τ_{br}	$B_{\mu G}$	$<$	$1.8 \times 10^{-4} n_0 E_{max}$
τ_{syn}	$B_{\mu G}$	$>$	$3400 E_{max}^{-2}$
Age-limited: $\tau_{acc}(E_{max}) > $ age	$B_{\mu G}$	$<$	$1.4 E_{max}$
Size-limited: $\frac{D(E_{max})}{v_{sh}} > \chi R_{sh}$	$B_{\mu G}$	$<$	$0.1 \chi_{0.1}^{-1} E_{max}$

Notes. $B_{\mu G}$, n_0 and the maximum particle energy E_{max} are in units of μG, cm^{-3} and TeV, respectively. The shock velocity $v_{sh} = 700$ km s^{-1} is used as it leads to conservative constraints on $B_{\mu G}$. The ratio between the diffusion length of particles at $E = E_{max}$ and the shock radius χ defines the upstream diffusion region size, where $\chi_{0.1} = \frac{\chi}{0.1}$ (e.g. Zirakashvili & Ptuskin 2008). τ_{p-p}, τ_{br} and τ_{syn} are the radiative loss timescales for p-p collision, Br and syn processes, τ_{acc} and τ_{rad} are the acceleration and radiative timescales, respectively, and $D(E_{max})$ the diffusion coefficient at the maximum energy.

In the age- and size-limited scenarios, the derived ULs on the magnetic field are lower than both the estimates of Hewitt et al. (2012), based on a simple one-zone modelling of Puppis A broadband emission (between 8 and 35 μG), and those of Dubner et al. (2013) and Arbutina et al. (2012), based on equipartition arguments (~ 26–$100 \mu G$). In other words, higher magnetic field values would have led to higher E_{max} and hence to VHE γ-ray emission from Puppis A detectable with the H.E.S.S. array. The ULs in Table 1 depend on the diffusion coefficient which could depart from the traditional Bohm assumption (see e.g. Parizot et al. 2006). However, strong deviations from the Bohm regime would be required to make the non-detection with H.E.S.S. compatible with the *Fermi*-LAT detection. In particular, for the hadronic scenario in the size-limited case, diffusion about two orders of magnitude slower than the Bohm one would be

---

[5] A toy model was used to study the coverage of this method by using Monte Carlo simulations. The results of these simulations indicate that the coverage is indeed fulfilled.

[6] By setting the coefficient k_0 from Eq. (14) of (Parizot et al. 2006) equal to unity.

needed. In the loss-limited cases due to p-p and Br interactions, lower limits on the density are much higher than that estimated from IR observations towards the NE rim ($\sim$4 cm^{-3}, Arendt et al. 2010), for any acceptable value of the magnetic field. Nonetheless, this density estimate, together with a realistic amount of energy in accelerated particles of $\sim$(1-4) $\times 10^{49}$ erg, can account for the GeV emission (Hewitt et al. 2012). The synchrotron limited case leads to a lower limit on the magnetic field far too high for a SNR of age $\sim$4500 yr. Hewitt et al. (2012) have treated E_{max} as a free parameter in their broadband modelling, fixing it to 0.5 (resp. 0.8) TeV in their leptonic (resp. hadronic) modelling in order not to violate the *Fermi*-LAT measurements, but without imposing any physical constraint. By applying the same reasoning as above with only these *Fermi*-LAT lower limits on E_{max}, non-constraining limits on $B_{\mu G}$ and n_0 are obtained.

The hypothesis of a break in the particle spectrum of Puppis A due to synchrotron losses results in a realistic lower limit on the magnetic field ($B_{\mu G} > 70\,E_{break}^{-1/2}$, E_{break} in TeV). However, leptonic-dominated scenarios would require an unusually high electron to proton ratio (larger than 0.1), in excess of the observed CR abundances (Hewitt et al. 2012). Radiative breaks due to p-p and Br mechanisms imply a constraint on $n_0 \gtrsim 10^4$ cm^{-3} much larger than the density estimates reported in Puppis A. Therefore, it turns out that none of the known limitations in the simple context of a single population of particles continuously accelerated at the SNR shock can explain the lack of VHE emission from the Puppis A SNR, except if the diffusion has been proceeding far from the Bohm limit.

However, if the SNR shock has encountered a MC some time ago, the acceleration of particles could have ceased due to ion-neutral damping. In such a case, a radiative cutoff would appear at an energy for which $\tau_{rad} = \Delta t$, with Δt the time elapsed since the beginning of the interaction. This would imply $n_0 \gtrsim 10^3$ cm^{-3} and $B \gtrsim 50\,\mu G$ for the Br/p-p and syn radiative losses, respectively. These values seem to be very reasonable for a MC (Crutcher 1999).

Alternatively, other scenarios that could explain a break in the HE regime deal with particle escape and diffusion in SNRs (e.g. Ohira et al. 2010; Malkov et al. 2012). Although these spectral breaks are generally observed at energies of $\sim$1$-$20 GeV (Abdo et al. 2009, 2010a,b,c,d), lower than the constraints presented here, it is not clear whether the detection of such breaks in this energy range is entirely due to a *Fermi*-LAT statistical selection effect or not. Some localised regions along the Puppis A outer rim are known to have interacted with dense surrounding material (such as the BEK, Hwang et al. 2005), but due to their very small sizes and positions along the SNR rim they may not be representative of the bulk of the GeV emission observed with *Fermi*-LAT. The GeV emission is more compatible with the (hard) X-ray morphology shown in Dubner et al. (2013) pointing towards the NE region adjacent to a cloud traced in the far-IR domain that is either yet to be hit or already being shocked by the Puppis A SNR. Such a cloud interaction could be responsible for a break in the HE/VHE γ-ray spectrum through the abovementioned mechanisms, but at somewhat higher energies than observed in the more evolved interacting SNRs.

4. Conclusion

The H.E.S.S. observations of Puppis A in the VHE domain reveal an unexpected lack of emission from the SNR. The extrapolation from the *Fermi*-LAT HE power-law spectrum to the VHE domain contrasts with the absence of VHE emission. The comparison of these two measurements indicates that a spectral feature (a break or a cutoff) must exist at energies around a few hundred GeV. By assuming a PL with an exponential (resp. subexponential) cutoff, such a feature should occur below 450 GeV (resp. 280 GeV) at the 99% CL. The latter value provides a conservative UL on any break energy as long as $\Delta\Gamma \lesssim 1$. In the context of a single population of particles continuously accelerated at the SNR forward shock through an on-going DSA process, and under the assumption of Bohm diffusion, it is difficult to reconcile the constraints on the magnetic field and ISM density derived from the broadband emission modelling (Hewitt et al. 2012) with those obtained here based on the predicted maximum/break particle energies. However, multi-wavelength data suggest that Puppis A has already interacted with MCs in some localised regions along the shell and that the NE region coincident with the bulk of GeV emission is possibly interacting with a far-IR MC (Dubner et al. 2013). If this is true, the acceleration of particles could have ceased some time ago, and either a radiative cutoff or a break of non-radiative origin could be expected. In the latter case, the break is expected at somewhat higher energies than those measured in several SNRs known to be interacting with MCs, which lie in the 1-20 GeV energy range (Abdo et al. 2009, 2010d,a; Ackermann et al. 2013). Upcoming observations with the five-telescope H.E.S.S. II will allow the unexplored $\sim$100$-$300 GeV domain, where this spectral feature is predicted to exist, to be probed for the first time.

References

Abdo, A. A., Ackermann, M., Ajello, M., et al. 2011, ApJ, 734, 28
Abdo, A. A., Ackermann, M., Ajello, M., et al. 2010a, ApJ, 718, 348
Abdo, A. A., Ackermann, M., Ajello, M., et al. 2009, ApJ, 706, L1
Abdo, A. A., Ackermann, M., Ajello, M., et al. 2010b, Science, 327, 1103
Abdo, A. A., Ackermann, M., Ajello, M., et al. 2010c, ApJ, 712, 459
Abdo, A. A., Ackermann, M., Ajello, M., et al. 2010d, ApJ, 722, 1303
Abramowski, A., Acero, F., Aharonian, F., et al. 2012, A&A, 548, A38
Ackermann, M., Ajello, M., Allafort, A., et al. 2013, Science, 339, 807
Aharonian, F., Akhperjanian, A. G., Bazer-Bachi, A. R., et al. 2008, A&A, 481, 401
Aharonian, F., Akhperjanian, A. G., Bazer-Bachi, A. R., et al. 2006a, A&A, 457, 899
Aharonian, F., Akhperjanian, A. G., Bazer-Bachi, A. R., et al. 2006b, A&A, 448, L43
Aharonian, F., Akhperjanian, A. G., Bazer-Bachi, A. R., et al. 2007, A&A, 464, 235
Albert, J., Aliu, E., Anderhub, H., et al. 2007, ApJ, 664, L87
Arbutina, B., Urošević, D., Andjelić, M. M., Pavlović, M. Z., & Vukotić, B. 2012, ApJ, 746, 79
Arendt, R. G., Dwek, E., Blair, W. P., et al. 2010, ApJ, 725, 585
Becker, W., Prinz, T., Winkler, P. F., & Petre, R. 2012, ApJ, 755, 141
Bell, A. R. 1978a, MNRAS, 182, 147
Bell, A. R. 1978b, MNRAS, 182, 443
Berge, D., Funk, S., & Hinton, J. 2007, A&A, 466, 1219
Bernlöhr, K., Carrol, O., Cornils, R., et al. 2003, Astroparticle Physics, 20, 111
Blandford, R. D. & Ostriker, J. P. 1978, ApJ, 221, L29
Castelletti, G., Dubner, G., Golap, K., & Goss, W. M. 2006, A&A, 459, 535
Chevalier, R. A. 1977, ARA&A, 15, 175
Crutcher, R. M. 1999, ApJ, 520, 706
de Naurois, M. & Rolland, L. 2009, Astroparticle Physics, 32, 231

Dubner, G., Loiseau, N., Rodríguez-Pascual, P., et al. 2013, A&A, 555, A9

Dubner, G. M. & Arnal, E. M. 1988, A&AS, 75, 363

Feldman, G. J. & Cousins, R. D. 1998, Phys. Rev. D, 57, 3873

Gabici, S., Aharonian, F. A., & Casanova, S. 2009, MNRAS, 396, 1629

Ginzburg, V. L. & Syrovatskii, S. I. 1964, Soviet Ast., 8, 342

Hewitt, J. W., Grondin, M.-H., Lemoine-Goumard, M., et al. 2012, ApJ, 759, 89

Hwang, U., Flanagan, K. A., & Petre, R. 2005, ApJ, 635, 355

Hwang, U., Petre, R., & Flanagan, K. A. 2008, ApJ, 676, 378

Katsuda, S., Hwang, U., Petre, R., et al. 2010, ApJ, 714, 1725

Katsuda, S., Mori, K., Tsunemi, H., et al. 2008, ApJ, 678, 297

Katsuda, S., Ohira, Y., Mori, K., et al. 2013, ApJ, 768, 182

Kelner, S. R., Aharonian, F. A., & Bugayov, V. V. 2006, Phys. Rev. D, 74, 034018

Krymskii, G. F. 1977, Soviet Physics Doklady, 22, 327

Lazendic, J. S., Wardle, M., Whiteoak, J. B., Burton, M. G., & Green, A. J. 2010, MNRAS, 409, 371

Lee, S.-H., Ellison, D. C., & Nagataki, S. 2012, ApJ, 750, 156

Li, T.-P. & Ma, Y.-Q. 1983, ApJ, 272, 317

Malkov, M. A., Diamond, P. H., & Sagdeev, R. Z. 2012, Physics of Plasmas, 19, 082901

Ohira, Y., Murase, K., & Yamazaki, R. 2010, A&A, 513, A17

Ohm, S., van Eldik, C., & Egberts, K. 2009, Astroparticle Physics, 31, 383

Parizot, E., Marcowith, A., Ballet, J., & Gallant, Y. A. 2006, A&A, 453, 387

Reichardt, I., de Oña-Wilhelmi, E., Rico, J., & Yang, R. 2012, A&A, 546, A21

Reynolds, S. P. 2008, ARA&A, 46, 89

Reynoso, E. M., Dubner, G. M., Goss, W. M., & Arnal, E. M. 1995, AJ, 110, 318

Reynoso, E. M., Green, A. J., Johnston, S., et al. 2003, MNRAS, 345, 671

Rolke, W. A., López, A. M., & Conrad, J. 2005, Nuclear Instruments and Methods in Physics Research A, 551, 493

Winkler, P. F. & Kirshner, R. P. 1985, ApJ, 299, 981

Woermann, B., Gaylard, M. J., & Otrupcek, R. 2000, MNRAS, 317, 421

Zirakashvili, V. N. & Aharonian, F. 2007, A&A, 465, 695

Zirakashvili, V. N. & Ptuskin, V. S. 2008, ApJ, 678, 939

[1] Universität Hamburg, Institut für Experimentalphysik, Luruper Chaussee 149, D 22761 Hamburg, Germany

[2] Max-Planck-Institut für Kernphysik, P.O. Box 103980, D 69029 Heidelberg, Germany

[3] Dublin Institute for Advanced Studies, 31 Fitzwilliam Place, Dublin 2, Ireland

[4] National Academy of Sciences of the Republic of Armenia, Marshall Baghramian Avenue, 24, 0019 Yerevan, Republic of Armenia

[5] Yerevan Physics Institute, 2 Alikhanian Brothers St., 375036 Yerevan, Armenia

[6] Institut für Physik, Humboldt-Universität zu Berlin, Newtonstr. 15, D 12489 Berlin, Germany

[7] University of Namibia, Department of Physics, Private Bag 13301, Windhoek, Namibia

[8] University of Durham, Department of Physics, South Road, Durham DH1 3LE, U.K.

[9] GRAPPA, Anton Pannekoek Institute for Astronomy, University of Amsterdam, Science Park 904, 1098 XH Amsterdam, The Netherlands

[10] Obserwatorium Astronomiczne, Uniwersytet Jagielloński, ul. Orla 171, 30-244 Kraków, Poland

[11] now at Harvard-Smithsonian Center for Astrophysics, 60 Garden St, MS-20, Cambridge, MA 02138, USA

[12] Department of Physics and Electrical Engineering, Linnaeus University, 351 95 Växjö, Sweden

[13] Institut für Theoretische Physik, Lehrstuhl IV: Weltraum und Astrophysik, Ruhr-Universität Bochum, D 44780 Bochum, Germany

[14] GRAPPA, Anton Pannekoek Institute for Astronomy and Institute of High-Energy Physics, University of Amsterdam, Science Park 904, 1098 XH Amsterdam, The Netherlands

[15] Institut für Astro- und Teilchenphysik, Leopold-Franzens-Universität Innsbruck, A-6020 Innsbruck, Austria

[16] Laboratoire Leprince-Ringuet, Ecole Polytechnique, CNRS/IN2P3, F-91128 Palaiseau, France

[17] now at Santa Cruz Institute for Particle Physics, Department of Physics, University of California at Santa Cruz, Santa Cruz, CA 95064, USA

[18] Centre for Space Research, North-West University, Potchefstroom 2520, South Africa

[19] LUTH, Observatoire de Paris, CNRS, Université Paris Diderot, 5 Place Jules Janssen, 92190 Meudon, France

[20] LPNHE, Université Pierre et Marie Curie Paris 6, Université Denis Diderot Paris 7, CNRS/IN2P3, 4 Place Jussieu, F-75252, Paris Cedex 5, France

[21] Institut für Astronomie und Astrophysik, Universität Tübingen, Sand 1, D 72076 Tübingen, Germany

[22] Laboratoire Univers et Particules de Montpellier, Université Montpellier 2, CNRS/IN2P3, CC 72, Place Eugène Bataillon, F-34095 Montpellier Cedex 5, France

[23] DSM/Irfu, CEA Saclay, F-91191 Gif-Sur-Yvette Cedex, France

[24] Astronomical Observatory, The University of Warsaw, Al. Ujazdowskie 4, 00-478 Warsaw, Poland

[25] Instytut Fizyki Jądrowej PAN, ul. Radzikowskiego 152, 31-342 Kraków, Poland

[26] School of Physics, University of the Witwatersrand, 1 Jan Smuts Avenue, Braamfontein, Johannesburg, 2050 South Africa

[27] Landessternwarte, Universität Heidelberg, Königstuhl, D 69117 Heidelberg, Germany

[28] Oskar Klein Centre, Department of Physics, Stockholm University, Albanova University Center, SE-10691 Stockholm, Sweden

[29] Wallenberg Academy Fellow,

[30] School of Chemistry & Physics, University of Adelaide, Adelaide 5005, Australia

[31] APC, AstroParticule et Cosmologie, Université Paris Diderot, CNRS/IN2P3, CEA/Irfu, Observatoire de Paris, Sorbonne Paris

Cité, 10, rue Alice Domon et Léonie Duquet, 75205 Paris Cedex 13, France

[32] Univ. Grenoble Alpes, IPAG, F-38000 Grenoble, France
CNRS, IPAG, F-38000 Grenoble, France

[33] Department of Physics and Astronomy, The University of Leicester, University Road, Leicester, LE1 7RH, United Kingdom

[34] Nicolaus Copernicus Astronomical Center, ul. Bartycka 18, 00-716 Warsaw, Poland

[35] Institut für Physik und Astronomie, Universität Potsdam, Karl-Liebknecht-Strasse 24/25, D 14476 Potsdam, Germany

[36] Laboratoire d'Annecy-le-Vieux de Physique des Particules, Université de Savoie, CNRS/IN2P3, F-74941 Annecy-le-Vieux, France

[37] DESY, D-15738 Zeuthen, Germany

[38] Université Bordeaux 1, CNRS/IN2P3, Centre d'Études Nucléaires de Bordeaux Gradignan, 33175 Gradignan, France

[39] Universität Erlangen-Nürnberg, Physikalisches Institut, Erwin-Rommel-Str. 1, D 91058 Erlangen, Germany

[40] Centre for Astronomy, Faculty of Physics, Astronomy and Informatics, Nicolaus Copernicus University, Grudziadzka 5, 87-100 Torun, Poland

[41] Funded by contract ERC-StG-259391 from the European Community,

[42] Department of Physics, University of the Free State, PO Box 339, Bloemfontein 9300, South Africa

[43] GRAPPA, Institute of High-Energy Physics, University of Amsterdam, Science Park 904, 1098 XH Amsterdam, The Netherlands